10 March 2000

ELSEVIER

Chemical Physics Letters 319 (2000) 113–118

CHEMICAL PHYSICS LETTERS

www.elsevier.nl/locate/cplett

Photoluminescence intensity and anisotropy decays in amorphous carbon

M.N. Berberan-Santos [a], A. Fedorov [a], J.P. Conde [b], C. Godet [c,*], T. Heitz [c], J.E. Bourée [c]

[a] *Centro de Química-Física Molecular, Instituto Superior Técnico, Av. Rovisco Pais, 1049-001 Lisboa, Portugal*
[b] *Department of Materials Engineering, Instituto Superior Tecnico, Av. Rovisco Pais, 1049-001 Lisboa, Portugal*
[c] *Laboratoire de Physique des Interfaces et des Couches Minces (UMR 7647 CNRS), Ecole Polytechnique, 91128 Palaiseau Cedex, France*

Received 1 November 1999; in final form 21 December 1999

Abstract

The decays of intensity and anisotropy of UV-excited photoluminescence (PL) in hydrogenated amorphous carbon have been investigated in the ps–ns time range. For emission energies E_{em} between 1.8 and 3.5 eV, anisotropy decreases within 100 ps and reaches a plateau within 1 ns. The emission anisotropy plateau value increases (from 0.02 to 0.12) and the decay time of PL intensity decreases (from 1 ns to 40 ps) as E_{em} increases. The exponential increase of time-averaged anisotropy as E_{em} increases is explained by a competition between exciton decay and randomization of polarization due to electronic excitation energy transfer (Förster mechanism) between chromophores. © 2000 Elsevier Science B.V. All rights reserved.

1. Introduction

Bulk and thin film π-bonded materials have attracted a lot of attention for their peculiar electronic properties (such as fast response, nonlinear optical behaviour and polarized photoluminescence) in particular those arising from conjugated systems in quantum wires or fullerenes.

In order to contribute to understanding the polarization of photoluminescence in π-bonded materials, we have performed picosecond time-resolved studies of carbon thin films. In contrast with crystalline organic polymers which usually provide narrow excitonic lines in absorption and photoluminescence (PL) spectra, polymer-like hydrogenated amorphous carbon (a-C:H) films exhibit a broad emission covering the whole visible range [1–5] corresponding to electronic transitions between π (HOMO) and π* (LUMO) molecular orbitals. Some confinement of photogenerated electron–hole pairs inside π-bonded 'grains' has been inferred from the lack of thermal quenching, the fast (subnanosecond) exciton-like decay of PL intensity [1] and from the constant decay time as a function of generation rate [6].

This Letter confirms earlier studies of plasma-deposited carbon-rich a-Si_xC_{1-x}:H [7] or a-C:H [4,5] films showing a significant degree of polarization memory for cw-PL excited with linearly polarized light. In order to explain the time-resolved measure-

* Corresponding author. Fax: +33-1-69-33-30-06; e-mail: godet@poly.polytechnique.fr

0009-2614/00/$ - see front matter
PII: S0009-2614(00)00102-0

ments presented in this Letter, giving evidence of a fast decrease of emission anisotropy towards a finite plateau value between 0.1 and 1 ns, a dipole–dipole electronic excitation energy transfer (or Förster mechanism) is proposed rather than previous descriptions based on phonon-assisted depolarization.

2. Experimental

Time-averaged and time-resolved behavior of photoluminescence are investigated using a polymer-like a-C:H film (43 H at%, density 1.6 g cm^{-3}) grown on crystalline silicon using a dual-plasma process [8], which is typical of amorphous carbon with high PL efficiency. The carbon films are amorphous, as shown by the broad C–C pair correlation functions deduced from X-ray diffraction [9]. Absorption at excitation energy $E_{exc} = 4.13$ eV (300 nm) is homogeneous, the film thickness (190 nm) being smaller than the absorption depth (430 nm) as deduced from spectroscopic ellipsometry [8].

Time-averaged PL measurements were performed at 300 K with a SPEX Fluorolog system. UV light from a Xe arc lamp was focused onto the sample (incidence angle $\sim 60°$) through a monochromator set at 300 nm (27 nm excitation bandwidth). The resulting PL was collected by a monochromator (9 nm emission bandwidth) coupled with a photomultiplier. Polarized spectra were recorded in the V–V, V–H, H–V and H–H configurations (H corresponding to the plane of incidence) with 20 s integration time, a bandpass filter 250–400 nm being inserted between the first polarizer and the carbon film. The photomultiplier background level was subtracted before calculation of the time-averaged anisotropy $\langle r \rangle$ [10]:

$$\langle r \rangle = (I_{\parallel} - I_{\perp})/(I_{\parallel} + 2I_{\perp}) = (I_{VV}/k - I_{VH})/(I_{VV}/k + 2I_{VH}), \quad (1)$$

where $k = (I_{HV}/I_{HH})$ is introduced to take into account the polarization response of the monochromator.

The dynamic relaxation of photo-excited carriers has been investigated at 300 K using laser excitation at 4.13 eV (300 nm) and 2.15 eV (577 nm). In the latter case, complementary data were collected at 300 and 80 K. Picosecond time-resolved PL decays were obtained by the single-photon timing method, with excitation from a Coherent 701-2 dye laser, delivering 3–4 ps pulses (~ 40 nJ/pulse) at a frequency of 3.4 MHz. The instrument response function has an effective FWHM of 30 ps. Time scales varied between 0.955 ps/channel and 5.52 ps/channel, with 1024 acquisition channels. Intensity decay measurements were made by alternated collection of impulses and decays with the emission polarizer set either at magic angle position (unpolarized PL) or at H (respectively V) position. Detection by a microchannel plate photomultiplier was done by passing the emission through a depolarizer and then through a monochromator. Data reported here were taken with incidence and emission angles of 15° and 0°, respectively, but qualitatively similar results were obtained with the 74°–16° configuration.

3. Results

Fig. 1 shows the broad total PL emission spectra, along with the time-averaged anisotropy $\langle r \rangle$. As emission energy E_{em} decreases in the range 2.2–3.0 eV, an exponential decrease of $\langle r \rangle$ is evidenced. For E_{em} lower than 1.9 eV, the signal-to-noise ratio is too low to measure $\langle r \rangle$ therefore $\langle r \rangle$ has been extrapolated as shown in Fig. 1b.

Fig. 2 shows typical experimental decays of intensity and emission anisotropy for PL emission at $E_{em} = 2.95$ eV (420 nm) excited at $E_{exc} = 4.13$ eV (300 nm). Intensity decays have been fitted using a convolution between the laser excitation and an analytic intrinsic decay function. Although a continuous distribution of PL decay times could be expected from an amorphous material, the assumption of a discrete distribution of decay times has been made. The experimental data are very accurately fitted using a decay function made of the sum of three exponentials (6-parameter fit) as shown in Fig. 2a. The decay times (τ_1) of PL intensity are obtained as a weighted average of the fitted decay times. They decrease from 965 to 39 ps as a function of increasing emission energy E_{em} (Table 1).

As illustrated in Fig. 2b, for 4.13 eV excitation, PL emission anisotropy decreases from ~ 0.30 within ~ 100 ps, independently of E_{em}. Within

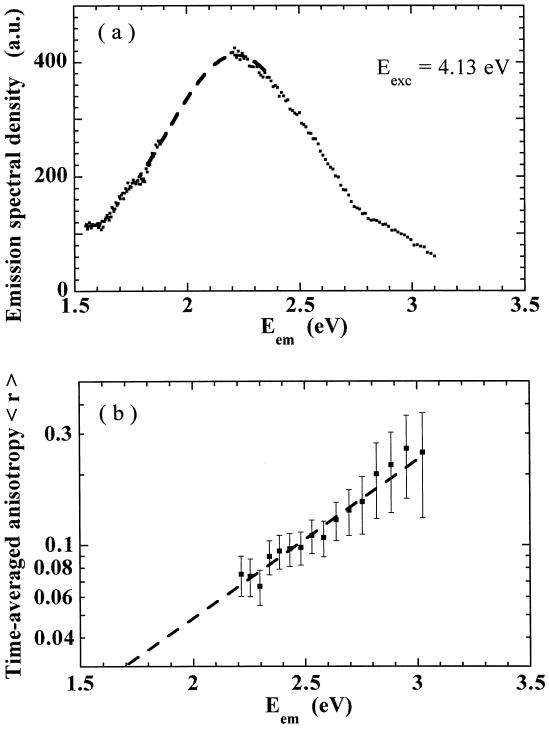

Fig. 1. (a) Spectral density of PL emission at room temperature ($E_{exc} = 4.13$ eV). Dashed lines indicate interpolation of data in the excitation second order near 2.1 eV. (b) Time-averaged anisotropy $\langle r \rangle$ of PL. Dashed lines indicate extrapolated values.

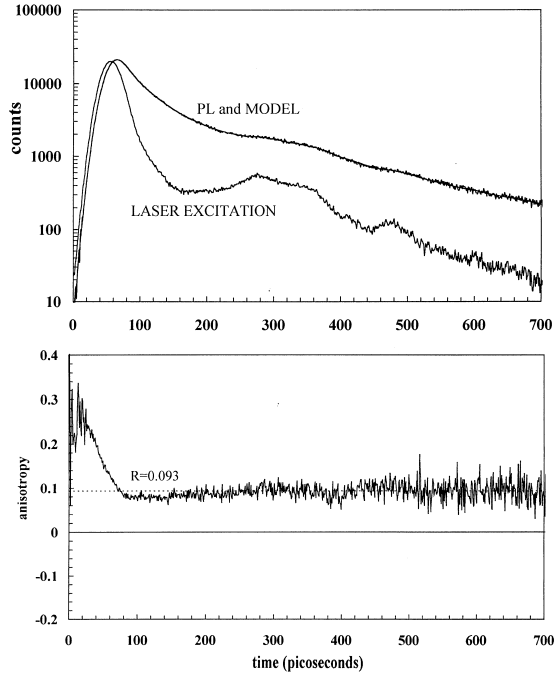

Fig. 2. (a) PL intensity decay at $E_{em} = 2.95$ eV using $E_{exc} = 4.13$ eV excitation (the time dependence of the laser excitation is also shown). The fitted 3-exponential decay is superimposed to experimental data. (b) Anisotropy decay: the plateau value ($r = 0.093$) is fitted between 200 and 700 ps. The time scale was 0.955 ps/channel.

200–1000 ps, the anisotropy reaches a plateau with a finite value (noted $r(1\,\mathrm{ns})$) which increases from 0.02 to 0.12 as a function of increasing emission energy. Plateau values as large as 0.21 ± 0.02 (300 K) or 0.24 ± 0.03 (80 K) have been obtained for 1.75 eV emission, excited at lower energy $E_{exc} = 2.15$ eV. The anisotropy decay function is quite complex and its description remains beyond the scope of this investigation.

A coherent picture of time-averaged and time-resolved anisotropy values can be obtained from a simple description taking into account the measured time-dependent generation rate $L(t)$ due to laser beam absorption and assuming a single-exponential decay of PL intensity: $f(t) = \exp(-t/\tau_d)$ and a single-exponential function for the anisotropy decay: $r(t) = r_\infty + (r_0 - r_\infty)\exp(-t/\tau_{DP})$. One obtains for the time-averaged polarization anisotropy

$$\langle r \rangle = \left[r_\infty + r_0(\tau_{DP}/\tau_d) \right] / \left[1 + (\tau_{DP}/\tau_d) \right], \qquad (2)$$

giving the average depolarization time

$$\tau_{DP} = (\nu_{DP})^{-1} = \tau_d \left[\langle r \rangle - r_\infty \right] / \left[r_0 - \langle r \rangle \right]. \qquad (3)$$

Assuming the highest physical value of polarization anisotropy $r_0 = 0.40$ (a lower value of 0.30 being

Table 1
Some measured PL characteristics of amorphous carbon using $E_{exc} = 4.13$ eV: time-averaged anisotropy $\langle r \rangle$, intensity decay time (τ_I) and anisotropy plateau value $r(1\,\mathrm{ns})$
Using the assumed initial anisotropy r_0, a calculated anisotropy decay time ($\tau_{DP\,calc}$) is obtained from (Eq. (3))

λ_{em} (nm)	E_{em} (eV)	τ_I (ps)	r_0	$r(1\,\mathrm{ns})$	$\langle r \rangle$	$\tau_{DP\,calc}$ (ps)	$\tau_{DP\,calc}/\tau_I$
350	3.54	39	0.40	0.120	0.25[a]	34	0.87
420	2.95	90	0.40	0.093	0.258	105	1.16
470	2.64	204	0.40	0.080	0.127	35	0.17
545	2.28	541	0.40	0.041	0.076	59	0.11
700	1.77	965	0.40	0.025	0.035[a]	26	0.03

[a] Extrapolated ± 0.05 (Fig. 1b).

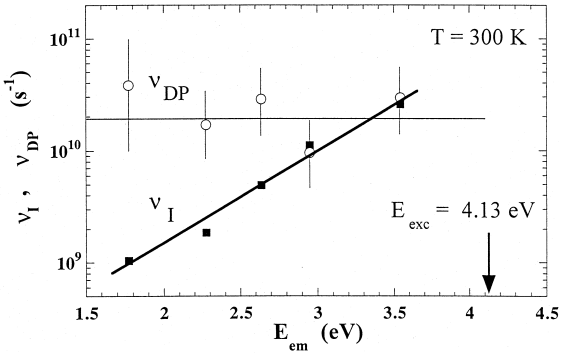

Fig. 3. Intensity decay rate (ν_I) and depolarization rate (ν_{DP}) dependence on the emission energy ($E_{exc} = 4.13$ eV).

obtained experimentally in Fig. 2b), using $r_\infty = r(1$ ns) and $\langle r \rangle$ values shown in Fig. 1b, one obtains values of $(\nu_{DP}) \approx 2 \times 10^{10}$ s^{-1} which remain basically independent on E_{em} in the range 1.8–3.5 eV (Table 1).

Fig. 3 shows the respective behavior of the depolarization rate (ν_{DP}) and the intrinsic decay rate (ν_I) as a function of emission energy E_{em}. Their ratio changes by more than one order of magnitude and explains the E_{em}-dependence of time-averaged anisotropy $\langle r \rangle$ on the basis of competing mechanisms. For emission energies below 2.7 eV, the intensity decay time (τ_I) is large, as compared to the depolarization time ($\tau_{DP} \approx 50$ ps), and the radiative recombination is weakly polarized. For higher E_{em} values ($E_{em} \geq 3.0$ eV) $\tau_I \approx \tau_{DP}$, corresponding to strongly polarized emission. In the following, the physical signification of the intensity decay rate (ν_I) and the depolarization rate (ν_{DP}) is addressed.

4. Discussion

The emission energy dependence of intrinsic PL decay rates, due to both radiative and non-radiative recombination mechanisms, is in quantitative agreement with previous studies of amorphous carbon films [2,6] and C-rich silicon carbon alloys with wide bandgap [11]. This result thus reveals a general behavior of π-bonded amorphous carbon films.

The observed subnanosecond decay times indicate that photogenerated pairs in a-C:H remain in close Coulomb interaction, in contrast with radiative tunneling recombination in a-Si:H which occurs in the μs–ms time range between carriers trapped separately in localized valence and conduction band tail states. As a consequence, previous models developed for PL in a-Si:H, where no polarization anisotropy has been reported, are unappropriate to describe or predict the PL properties of a-C:H.

Following the model developed by Kivelson et al. for trapped-exciton recombination in disordered solids [12], we assume that pair dissociation or radiative recombination only occurs after a fast thermalization of the exciton-like pair corresponding to relaxation of the excess energy by phonon emission within typically 1 ps. If the thermalized exciton is in thermal equilibrium with its surroundings, the dynamic characteristics of PL should be excitation energy independent. To assess the role of excitation energy and measurement temperature on carrier relaxation, intrinsic decay rates were measured at 300 and 80 K. For E_{em} values between 1.75 and 2.07 eV, the decay rates are found to be independent of measurement temperature (0.78–0.92 ns at 80 K, 0.66–0.78 ns at 300 K, using $E_{exc} = 2.15$ eV) and excitation energy (0.7–1 ns at 2.15 eV, 0.96 ns at 4.13 eV, measured at 300 K).

The fact that a broad asymmetrical emission band is observed, indicates the existence of a quasi-continuum of chromophores, each with its own manifold of states and characteristic emission spectrum and lifetime. The existence of resonance features in PL excitation spectra in a-C:H films [3] points towards the photogeneration of trapped excitons in which one of the charge carriers is trapped in a highly localized state in the pseudogap and the other carrier is bound to the first by their mutual Coulomb interaction in a large hydrogenic state. Exciton dissociation in amorphous carbon films appears to have a low probability since neither thermal (up to 300 K) nor electric field (up to 10^6 V cm^{-1}) quenching of PL, could be detected [1]. This is consistent with the very low photoconductivity of a-C:H.

Denser carbon films with lower bandgaps have smaller PL efficiencies because geometrical distortions of the carbon matrix may contribute to mixing of π and σ states, thus decreasing the confinement of photogenerated exciton-like pairs and enhancing non-radiative tunneling mechanisms. Non-radiative

decay also explains the shorter intrinsic decay time (τ_I) at higher E_{em} (Fig. 3): the decay rate becomes smaller at lower E_{em} where the density of available sites near midgap is smaller, eventually approaching the radiative decay rate. It is interesting to note that the decay time for the red chromophores is similar to the value measured for the most abundant fullerene, C_{60} (1.1 ns), a π-system known to emit in the same wavelength range [13].

A possible depolarization mechanism, often reported in polymers, is radiationless excitation transfer from a donor to an acceptor chromophore via incoherent resonant dipole–dipole interactions (Förster mechanism) [14,15]. For each transfer the depolarization efficiency is $\sim 96\%$ in a random medium. Chromophores may act as both donors or acceptors depending on the energetics.

The following features are expected from a radiationless energy transfer mechanism:

(1) The PL emission anisotropy will result, at all emission energies, from the directly excited high-energy chromophores (donors), the only ones to have polarized emission.

(2) The anisotropy plateau at longer times reflects the contribution to the PL of directly excited chromophores that have no acceptors in their neighbourhood. This contribution is expected to be smaller at lower emission energies where the emission of acceptors is dominant.

(3) Increasing excitation energy selects chromophores higher in the density of states distribution, providing a higher density of neighbouring chromophores that can act as acceptors. In this case, the anisotropy decay is fast and the plateau value is low. In contrast, excitation at lower energies selects donors that are surrounded by chromophores that cannot, in part, act as acceptors because their energies are likely to be higher than the primarily excited donors. In this way, the plateau value should be higher. All the described trends are observed.

As predicted by the model, the decay rate of anisotropy either coincides, or is faster than the decay rate of high-energy donors (Fig. 3).

In order to check for the Förster depolarization mechanism, a numerical estimate of the depolarization rate can be obtained from the excitation transfer rate (ν), which is proportional to the energy overlap between the emission spectral density of donor sites and the absorption spectrum of acceptor sites, separated by a distance R and can be expressed as:

$$\nu = (1/\tau_I)(R_0/R)^6, \tag{4}$$

where the effective critical Förster radii, R_0, usually take values between 20 and 60 Å [14,15]. Assuming a random distribution of chromophores, the decay law of initially excited donors is known to be given by: $i(t) = \exp[-(t/\tau_F) - bt^{1/2}]$, where $b = 0.845\, n_A[\pi/\tau_F]^{1/2}$ and $n_A = \frac{4}{3}\pi N_A[R_0]^3$ is the number of acceptor molecules within a sphere of radius R_0. A fit of this equation to the PL intensity decay at 3.54 eV (not shown) gives $(\tau_F) = 214$ ps (intrinsic decay time of the blue chromophores) and $b = 0.019$ ps$^{-1/2}$, corresponding to densities N_A of acceptor molecules between 2.0×10^{17} and 5.5×10^{18} cm^{-3}. It is stressed that the Förster decay equation strictly applies to emission close to the excitation energy, corresponding to primarily excited blue chromophores, in contrast with lower emission energies which include a significant number of acceptors. Hence, a significant difference between the Förster times τ_F and the model-free τ_I values is expected.

In this model, the long-time plateau of the anisotropy at high E_{em} reflects the fraction of isolated chromophores which cannot transfer within the intrinsic lifetime. Using the value of $r(1\,\text{ns}) = 0.12$ at $E_{em} = 3.54$ eV, one obtains an estimate for the fraction of isolated chromophores, $p = 0.12/0.40 = 0.3$, since 0.4 is the maximum polarization anisotropy value. Assuming a random distribution, the probability that no nearest neighbours occur for distances smaller than R is given by $p = \exp(-\frac{4}{3}\pi N_A R^3)$, resulting in $N_A = -3 \ln p/4\pi R^3$. Non-radiative transfer will be negligible for $R \geq 2R_0$, corresponding to distances of 40–120 Å, depending on the value of R_0. From the above values, one obtains concentrations of acceptors between 1.6×10^{17} and 4.5×10^{18} cm^{-3}, in agreement with the previous estimate.

5. Conclusions

In summary, the dynamic properties of photoluminescence in amorphous carbon films appear to be independent of excitation energy and measurement temperature ($80\,\text{K} < T < 300\,\text{K}$) providing strong

support for exciton-like behaviour. For emission energies E_{em} between 1.8 and 3.5 eV, the PL emission anisotropy decays are explained by non-radiative energy transfer from thermalized, primarily excited donors, to acceptor chromophores with a typical density, $N_A \approx 1 \times 10^{18}$ cm^{-3}.

Previous descriptions [4,7] of PL anisotropy properties in carbon films have assumed a phonon-assisted depolarization mechanism. Although such a mechanism cannot be ruled out in amorphous carbon, it is emphasized that these models do not explain the large anisotropy values (~ 0.30) of PL near 1–10 ps, i.e. after thermalization by phonon emission is completed, and the evidence of a plateau at longer times (0.1–1 ns range). In contrast, a coherent picture of time-averaged and time-resolved PL emission anisotropy in a-C:H has been obtained using a depolarization rate of 2×10^{10} s^{-1}, independent of E_{em}. We still do not have a complete understanding of the factors leading to a constant depolarization rate as a function of emission energy. However, the exponential decrease of time-averaged emission anisotropy as E_{em} decreases is explained by a competition between intrinsic exciton decay (including both radiative and non-radiative decays) and a radiationless excitation transfer (dipole–dipole or Förster mechanism) leading to efficient randomization of the initially polarized excitation.

Acknowledgements

We are grateful to V. Chu (INESC, Lisbon) who contributed to the steady-state PL measurements. This work was supported by grants from the CNRS–ICCTI exchange program and by the project PRAXIS 3/3.1/MMA/1901/95. A. Fedorov was supported by an INVOTAN (ICCTI) grant.

References

[1] S.V. Chernyshov, E.I. Terukov, V. Vassilyev, A.S. Volkov, J. Non-Cryst. Solids 134 (1991) 218.
[2] J.E. Bourée, T. Heitz, C. Godet, B. Drévillon, J.P. Conde, V. Chu, M.N. Berberan-Santos, A. Fedorov, J. Non-Cryst. Solids 227–230 (1998) 574.
[3] T. Heitz, C. Godet, J.E. Bourée, B. Drévillon, J.P. Conde, Phys. Rev. B 60 (1999) 6045.
[4] Rusli, G.A.J. Amaratunga, J. Robertson, Phys. Rev. B 53 (1996) 1630.
[5] M. Koós, I. Pócsik, L. Tóth, J. Non-Cryst. Solids 164–166 (1993) 1151.
[6] W. Lormes, M. Hundhausen, L. Ley, J. Non-Cryst. Solids 227 (1998) 570.
[7] Y. Masumoto, H. Kunitomo, S. Shionoya, H. Munekata, H. Kukimoto, Solid State Commun. 51 (1984) 209.
[8] C. Godet, T. Heitz, J.E. Bourée, B. Drévillon, C. Clerc, J. Appl. Phys. 84 (1998) 3919.
[9] C. Godet, T. Heitz, J.E. Bourée, B. Bouchet, J. Dixmier, B. Drévillon, Solid State Commun. 111 (1999) 293.
[10] M.N. Berberan-Santos, Rev. Port. Quim. 3 (1996) 3.
[11] J.P. Conde, V. Chu, M.F. da Silva, A. Kling, Z. Dai, J.C. Soares, S. Arekat, A. Fedorov, M.N. Berberan-Santos, F. Giorgis, C.F. Pirri, J. Appl. Phys. 85 (1999) 3327.
[12] S. Kivelson, C.D. Gelatt, Phys. Rev. B 26 (1982) 4646.
[13] A. Fedorov, M.N. Berberan-Santos, J.P. Lefèvre, B. Valeur, Chem. Phys. Lett. 267 (1997) 467.
[14] T. Förster, Discuss. Faraday Soc. 27 (1959) 7.
[15] M.D. Galanin, Luminescence of Molecules and Crystals, Cambridge International Science, Cambridge, 1996.